Vol 16 No 10, October 2007
1009-1963/2007/16(10)/3138-08
Chinese Physics
© 2007 Chin. Phys. Soc.
and IOP Publishing Ltd

Brownian dynamics simulation of two confined colloidal particles*

He Dong-Hui(何冬慧)[a)†], Yang Tao(杨涛)[b)], Li Wei-Hua(李卫华)[c)], Zhang Qing-Lan(张磬兰)[d)], and Ma Hong-Ru(马红孺)[b)]

[a)] *School of Physics and Engineering, Sun Yat-sen University, Guangzhou* 510275, *China*
[b)] *Institute of Theoretical Physics, Shanghai Jiao Tong University, Shanghai* 200240, *China*
[c)] *Department of Physics and Astronomy, McMaster University, Hamilton, Ontario, L8S* 4*M*1, *Canada*
[d)] *School of Physics and Electrical Information Science, Ningxia University, Yinchuan* 750021, *China*

(Received 24 December 2006; revised manuscript received 12 April 2007)

The dynamics of two confined colloidal particles is studied by means of Brownian dynamics simulation. The auto-correlation function and cross-correlation function of the two colloidal spheres are computed by utilizing the formulae of hydrodynamic diffusion matrix expanded to different orders, as well as the accurate tensor through numerical algorithm. Furthermore, the numerical results are compared with the experimental results and the theoretical approximation. It is found that the relatively simple theoretical approximation gives good predictions when two spheres are far away from each other, but fails when the two spheres are very close.

Keywords: Brownian dynamics simulation, hydrodynamics interaction, Oseen tensor, Rotne–Prager tensor

PACC: 8270D

1. Introduction

Colloidal suspensions are complex systems where colloidal particles disperse in solvents. Each particle experiences the friction force with solvent, hydrodynamic interaction, and direct potential force. Hydrodynamic interaction is an interaction among colloidal particles mediated by the solvent, with the following picture: when a colloidal particle moves through a fluid, it influences the surrounding solvent and makes them move, which produces a fluid velocity field. The force exerted on the neighbouring particles by this velocity field is hydrodynamics interaction.[1] Such hydrodynamic interactions are ubiquitous in many physical, chemical and biological systems, including complex fluids, polymer and protein.[2] The hydrodynamic interactions have been extensively studied for a long time due to the fact that they play a very important role in colloidal dynamics and biological systems, and many significant results have been obtained. From the physical point of view, the Reynolds numbers of the solvents in colloidal suspensions and biological systems are very small, which means that the relevant problems can be treated under the limit of low-Reynolds-number. Low-Reynolds-number hydrodynamics is a field being widely and deeply studied, and important outcomes and progress therein have been concluded in Refs.[3–7].

In recent years, the relevant studies have focused on the force acting on the colloidal spheres and the preparation of colloidal crystals as well as on the phase separation of the colloidal suspensions, and many interesting results have been obtained through computer simulation[8] and experimental measurements.[9,10] One of the most effective methods to study the hydrodynamical properties of colloidal suspensions is Brownian dynamics simulation, which has been successfully used to solve many problems, such as sedimentation and absorption of the protein, as well as flocculation of the suspension and the emulsion, etc. In the last twenty years, this method has been applied to simulating the dynamical behaviour of biological systems and great progress has been made. Many researchers in the early days have used Brownian dynamics simulation to study the motion of a single Brownian particle in solution. The two-particle Fokker-Planck equation was first deduced by Mazo.[11] Later on, Deutch and Oppenheim[12] derived a generalized Langevin equation from the Liouville equation for N Brownian particles and n solvent par-

*Project supported by the National Natural Science Foundation of China (Grant Nos 10174041 and 10334020).
†Corresponding author. E-mail: dh.he@163.com

ticles; and from the Langevin equation they deduced the N particle Fokker–Planck equation. Subsequently, Ermak and McCammon[13] proposed a method of Brownian dynamics simulation for N Brownian particles with hydrodynamic interactions based on the Langevin equation, and also pointed out the conditions under which this method could be applied. In this paper, we compute the coordinate correlations of two confined colloidal particles in solution under low Reynolds number, from which the influence of the hydrodynamic interaction can be deduced.

2. Model and theoretical calculation

2.1. Brownian dynamics simulation

Since the mass and the size of the Brownian particles are much larger than those of the solvent molecules, the solvent can be regarded as the continuum fluid medium. Hence we introduce a stochastic force to describe the influence of the thermal fluctuation of solvent molecules on the Brownian particles, which leads to the Langevin equation for N Brownian particles. By using some approximations, we obtain the Brownian dynamics formula for solving the Langevin equation as[13]

$$\begin{aligned} \boldsymbol{r}_i = \boldsymbol{r}_i^0 &+ \sum_j \frac{\partial \boldsymbol{D}_{ij}^0}{\partial \boldsymbol{r}_j}\Delta t \\ &+ \sum_j \frac{\boldsymbol{D}_{ij}^0 \cdot \boldsymbol{F}_j^0}{k_{\mathrm{B}}T}\Delta t + \boldsymbol{R}_i\left(\Delta t\right), \end{aligned} \tag{1}$$

where $\boldsymbol{r}_i$ denotes the centre-of-mass coordinates of the ith particle, and $\boldsymbol{F}_i$ is the direct force acting on the ith colloidal particle by the solvent. $\boldsymbol{D}_{ij}$ is the $3N \times 3N$ translational diffusion tensor describing the hydrodynamic interaction between Brownian particles. Here '0' represents the initial time, and the explicit expression of $\boldsymbol{D}_{ij}$ will be given later. In practical computations, the time step must be taken to be much larger than the momentum relaxation time, i.e. $\Delta t \gg \dfrac{m_i D_0}{k_{\mathrm{B}}T}$, where $D_0 = \dfrac{k_{\mathrm{B}}T}{6\pi\eta a}$, with η being the solvent viscosity, and a being the sphere radius. Meanwhile, numerical accuracy requires that the maximum time step should be sufficiently small, so that the force acting on the particle and the gradient of the diffusion tensor are essentially constant within the particle displacement during Δt. Accordingly, by omitting the terms associated with the gradient of the diffusion tensor in Eq.(1), we rewrite Eq.(1) as the difference equation

$$\boldsymbol{r}_i = \boldsymbol{r}_i^0 + \sum_j \frac{\boldsymbol{D}_{ij}^0 \boldsymbol{F}_j^0}{k_{\mathrm{B}}T}\Delta t + \boldsymbol{R}_i(\Delta t), \tag{2}$$

where $\boldsymbol{R}_i(\Delta t)$ is the random displacement caused by the stochastic force exerted on the particle by the surrounding solvent, with a zero average value, and with the correlation being $\langle \boldsymbol{R}_i(\Delta t)\boldsymbol{R}_j(\Delta t)\rangle = 2\boldsymbol{D}_{ij}\Delta t$. In numerical computations, this random displacement can be realized by sampling with the Gaussian distribution

$$P(\boldsymbol{R}, \Delta t) \propto \exp\left(-\frac{1}{2\Delta t}\boldsymbol{R}_i D_{ij}^{-1}\boldsymbol{R}_j\right). \tag{3}$$

2.2. Diffusion tensor for two particles

Calculation of diffusion tensor is generally very complicated. However, there are some analytical results for a system with two particles. The diffusion tensor of two particles is given by

$$\frac{\boldsymbol{D}_{ij}}{D_0} = 6\pi a \begin{pmatrix} \boldsymbol{S}_{11} & \boldsymbol{S}_{12} \\ \boldsymbol{S}_{21} & \boldsymbol{S}_{22} \end{pmatrix},$$

with the self-diffusion coefficient $D_0 = \dfrac{k_{\mathrm{B}}T}{6\pi\eta a}$. S is the mobility matrix with the symmetry

$$S_{ij}^{\alpha\beta} = S_{ji}^{\beta\alpha}, \tag{4}$$

where the indices $i, j = 1, 2$ denote the particles, and $\alpha, \beta = x, y, z$ represent the three spatial coordinates. The mobility matrix is expressed as

$$\boldsymbol{S}_{ij} = x_{ij}\boldsymbol{d}\boldsymbol{d} + y_{ij}(\boldsymbol{I} - \boldsymbol{d}\boldsymbol{d}), \tag{5}$$

where

$$\boldsymbol{d} = (\boldsymbol{r}_2 - \boldsymbol{r}_1)/|\boldsymbol{r}_2 - \boldsymbol{r}_1|.$$

Here x_{ij} and y_{ij} are called mobility functions, which are the functions of the distance between two particles, $r_{12} = |\boldsymbol{r}_2 - \boldsymbol{r}_1|$. When two spheres are very close to each other, we may define a new variable $\xi = (r_{12} - 2a)/a$, thus x_{ij} and y_{ij} can be expanded in near field as[14]

$$6\pi a x_{ij} = d_{ij}^{(1)} + d_{ij}^{(2)}\xi + d_{ij}^{(3)}\xi^2 \ln\xi + d_{ij}^{(4)}\xi^2, \tag{6}$$

$$6\pi a y_{ij} = \frac{S_{ij}^{(1)}(\ln\xi^{-1})^2 + S_{ij}^{(2)}\ln\xi^{-1} + S_{ij}^{(3)}}{(\ln\xi^{-1})^2 + e^{(1)}\ln\xi^{-1} + e^{(2)}} + O\left(\xi(\ln\xi)^3\right), \tag{7}$$

where

$$d_{11}^{(1)} = 0.7750, \quad d_{11}^{(2)} = 0.930, \quad d_{11}^{(3)} = 0.900, \quad d_{11}^{(4)} = -2.685,$$
$$d_{12}^{(1)} = 0.7750, \quad d_{12}^{(2)} = -1.070, \quad d_{12}^{(3)} = -0.900, \quad d_{12}^{(4)} = 2.697,$$

$$S_{11}^{(1)} = 0.89056, \quad S_{11}^{(2)} = 5.77196, \quad S_{11}^{(3)} = 7.06897,$$
$$S_{12}^{(1)} = 0.48951, \quad S_{12}^{(2)} = 2.80545, \quad S_{12}^{(3)} = 1.98174,$$
$$e^{(1)} = 6.04250, \quad e^{(2)} = 6.32549.$$

On the other hand, when the interparticle distance is very large, x_{ij} and y_{ij} can be expanded in far field as[15]

$$6\pi a x_{11} = 1 - 60\left(\frac{a}{2r_{ij}}\right)^4 + 352\left(\frac{a}{2r_{ij}}\right)^6 + 2688\left(\frac{a}{2r_{ij}}\right)^8 - 85504\left(\frac{a}{2r_{ij}}\right)^{10} + O\left(\left(\frac{a}{2r_{ij}}\right)^{12}\right),$$

$$6\pi a x_{12} = 3\left(\frac{a}{2r_{ij}}\right) - 8\left(\frac{a}{2r_{ij}}\right)^3 + 2400\left(\frac{a}{2r_{ij}}\right)^7 - 3840\left(\frac{a}{2r_{ij}}\right)^9 - 201216\left(\frac{a}{2r_{ij}}\right)^{11} + O\left(\left(\frac{a}{2r_{ij}}\right)^{13}\right),$$

$$6\pi a y_{11} = 1 - 68\left(\frac{a}{2r_{ij}}\right)^6 - 320\left(\frac{a}{2r_{ij}}\right)^8 - 4416\left(\frac{a}{2r_{ij}}\right)^{10} + O\left(\left(\frac{a}{2r_{ij}}\right)^{12}\right),$$

$$6\pi a y_{12} = \frac{3}{2}\left(\frac{a}{2r_{ij}}\right) + 4\left(\frac{a}{2r_{ij}}\right)^3 + 9072\left(\frac{a}{2r_{ij}}\right)^{11} + O\left(\left(\frac{a}{2r_{ij}}\right)^{13}\right). \tag{8}$$

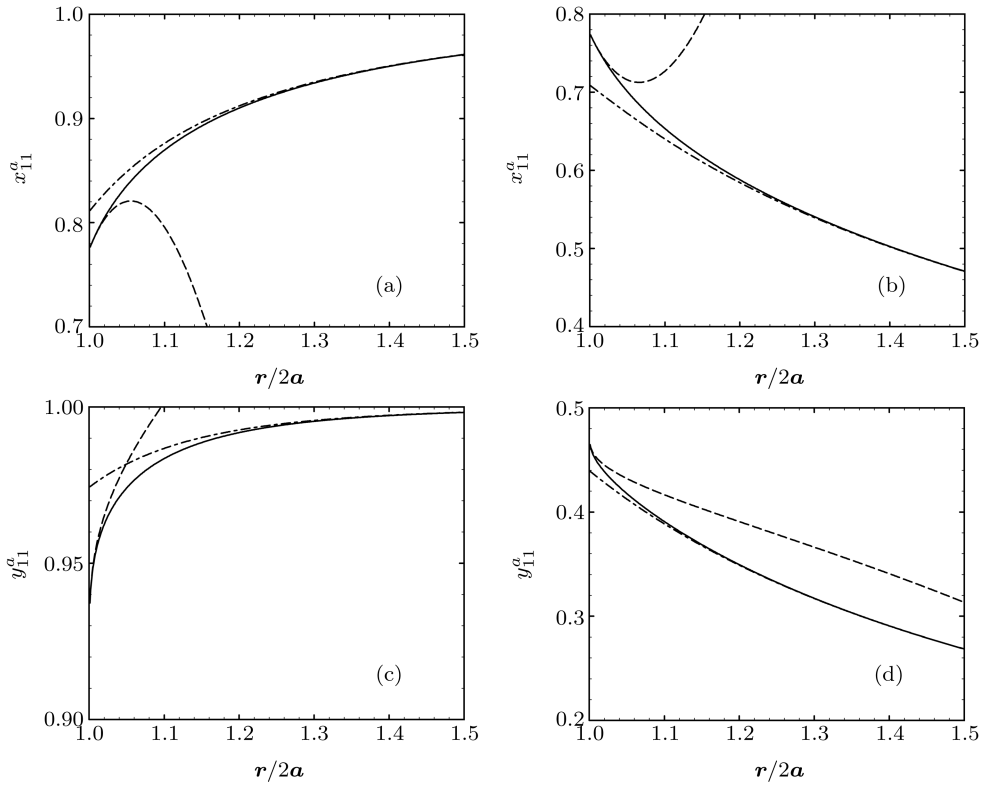


Fig.1. Values of the mobility function as a function of the distance between two colloid spheres. Dashed line corresponds to the near field formula, dot-dashed line the far field formula, and solid line the exact result from numerical calculations.

Using Eqs.(8), and retaining the first-order terms in $\frac{1}{r_{ij}}$, we arrive at the familiar Oseen tensor

$$\begin{aligned}\boldsymbol{D}_{ii} &= \frac{k_{\mathrm{B}}T}{6\pi\eta a}\boldsymbol{I},\\ \boldsymbol{D}_{ij} &= \frac{k_{\mathrm{B}}T}{8\pi r_{ij}\eta}\left(\boldsymbol{I}+\frac{\boldsymbol{r}_{ij}\boldsymbol{r}_{ij}}{r^2}\right).\end{aligned} \tag{9}$$

Similarly, retaining the third-order terms in $\frac{1}{r_{ij}}$ leads to the Rotne-Prager tensor

$$\begin{aligned}\boldsymbol{D}_{ii} &= \frac{k_{\mathrm{B}}T}{6\pi\eta a}\boldsymbol{I},\\ \boldsymbol{D}_{ij} &= \frac{k_{\mathrm{B}}T}{8\pi r_{ij}\eta}\left[\left(\boldsymbol{I}+\frac{\boldsymbol{r}_{ij}\boldsymbol{r}_{ij}}{r^2}\right)\right.\\ &\quad\left.+\frac{2a^2}{r_{ij}^2}\left(\frac{1}{3}\boldsymbol{I}-\frac{\boldsymbol{r}_{ij}\boldsymbol{r}_{ij}}{r^2}\right)\right].\end{aligned} \tag{10}$$

It is obvious that the two expressions given above do not describe exactly the diffusion tensor in all distances. However, Hinsen[16] provided the numerical method and algorithm for computing the mobility functions in all distances. Using Hinsen's program package, we compute the mobility function of two spheres and the results are shown in Fig.1. It can be seen that the two expansion expressions are consistent with the numerical results in small and large distances, respectively. However, they deviate from the numerical results in moderate distances.

2.3. Brownian dynamics simulation of two confined particles

In this paper we study a model where two colloidal spheres are confined within two small ranges by the optical tweezers, separately. The binding potential can be approximated by the harmonic oscillator potential, while there are no direct interactions between these two particles. This model accords with the experiment by Meiners and Quake[6] in 1999. If we take the equilibrium position of the first particle as the origin $(0,0)$, and situate the second particle at point $(E,0)$, the binding potential can be written as

$$U(\boldsymbol{r}_1)=\frac{1}{2}k\boldsymbol{r}_1^2,\quad\text{and}\quad U(\boldsymbol{r}_2)=\frac{1}{2}k(\boldsymbol{r}_1-E\hat{\boldsymbol{x}})^2,$$

where k is the strength of trap potential, and $\hat{\boldsymbol{x}}$ represents the unit vector in the x-direction. Thus, the Brownian dynamics formulae of the two colloidal particles are expressed as

$$\begin{aligned}\boldsymbol{r}_1(t+\Delta t) &= \boldsymbol{r}_1(t)+\frac{\boldsymbol{D}_{11}(\boldsymbol{r}_1(t)-\boldsymbol{r}_2(t))}{k_{\mathrm{B}}T}\cdot(-k\boldsymbol{r_1}(\boldsymbol{t}))\Delta t\\ &\quad+\frac{\boldsymbol{D}_{12}(\boldsymbol{r}_1(t)-\boldsymbol{r}_2(t))}{k_{\mathrm{B}}T}\cdot(-k(\boldsymbol{r}_2(t)-E\hat{\boldsymbol{x}}))\Delta t+\boldsymbol{R}_1(\Delta t),\\ \boldsymbol{r}_2(t+\Delta t) &= \boldsymbol{r}_2(t)+\frac{\boldsymbol{D}_{22}(\boldsymbol{r}_2(t)-\boldsymbol{r}_1(t))}{k_{\mathrm{B}}T}\cdot(-k\boldsymbol{r_1}(\boldsymbol{t}))\Delta t\\ &\quad+\frac{\boldsymbol{D}_{21}(\boldsymbol{r}_2(t)-\boldsymbol{r}_1(t))}{k_{\mathrm{B}}T}\cdot(-k(\boldsymbol{r}_2(t)-E\hat{\boldsymbol{x}}))\Delta t+\boldsymbol{R}_2(\Delta t),\end{aligned} \tag{11}$$

where $\boldsymbol{R}_1(\Delta t)$ and $\boldsymbol{R}_2(\Delta t)$ are the random displacements of two particles, respectively, which are determined by the distribution of Eq.(2). Equations (11) constitute the Brownian dynamics algorithm for calculating the motion of two confined colloidal spheres.

The trajectory of the colloid particle is a zigzag curve around its equilibrium position. We can extract the information of the motion through the correlation functions of the colloid particles. There are two kinds of the correlations we used here, i.e. the autocorrelation function and cross correlation function, referring to the correlation of the same colloid particle at different times and the correlation between the two colloid particles at different times, respectively. The autocorrelation function is defined as

$$C^{\alpha\beta}\tau=\langle r_i^{\alpha}(t+\tau)r_i^{\beta}(t)\rangle, \tag{12}$$

where i can be either 1 or 2, indicating particle 1 or particle 2, and the two particles have the same autocorrelation function in statistics. α and β index the spatial directions which take values x, y and z. The cross correlation function is defined as

$$C_{12}^{\alpha\beta}\tau=\langle r_1^{\alpha}(t+\tau)r_2^{\beta}(t)\rangle. \tag{13}$$

These two correlation functions are experimentally measurable quantities which contain the information about the binding potential and the viscosity of the fluid around the colloidal particles.

By omitting the higher-order terms of Δt, which is equivalent to taking the limit of $\Delta t \to 0$ to Eqs.(11), we define

$$\lim_{\Delta t\to 0} \frac{\boldsymbol{R}_i(\Delta t)}{\Delta t} = \boldsymbol{f}_i, \tag{14}$$

and finally arrive at the differential form of Eqs.(11) as

$$\begin{aligned}
\frac{\mathrm{d}\boldsymbol{r}_1}{\mathrm{d}t} &= -k\frac{\boldsymbol{D}_{11}(\boldsymbol{r}_1-\boldsymbol{r}_2)}{k_\mathrm{B}T}\cdot\boldsymbol{r_1} \\
&\quad -k\frac{\boldsymbol{D}_{12}(\boldsymbol{r}_1-\boldsymbol{r}_2)}{k_\mathrm{B}T}\cdot(\boldsymbol{r}_2-E\hat{\boldsymbol{x}})+\boldsymbol{f}_1\,, \\
\frac{\mathrm{d}\boldsymbol{r}_2}{\mathrm{d}t} &= -k\frac{\boldsymbol{D}_{21}(\boldsymbol{r}_2-\boldsymbol{r}_1)}{k_\mathrm{B}T}\cdot\boldsymbol{r_1} \\
&\quad -k\frac{\boldsymbol{D}_{22}(\boldsymbol{r}_2-\boldsymbol{r}_1)}{k_\mathrm{B}T}\cdot(\boldsymbol{r}_2-E\hat{\boldsymbol{x}})+\boldsymbol{f}_2\,.
\end{aligned} \tag{15}$$

It should be noted that the limit in Eq.(14) does not actually exist. The relation $\boldsymbol{R}_i(\Delta t) \sim \sqrt{\Delta t}$ leads to $\lim_{\Delta t\to 0} \frac{\boldsymbol{R}_i(\Delta t)}{\Delta t} \sim \frac{\sqrt{\Delta t}}{\Delta t} \to \frac{1}{\sqrt{\Delta t}}$, which implies that the above limit does not exist. In order to obtain accurate and self-consistent results in numerical calculations, we regard $\boldsymbol{f}_i(t)$ as a random variable, which satisfies

$$\begin{aligned}
&\langle \boldsymbol{f}_i(t)\rangle = 0, \\
&\langle \boldsymbol{f}_i(t)\boldsymbol{f}_j(t')\rangle = 2\boldsymbol{D}_{ij}\delta(t-t').
\end{aligned} \tag{16}$$

If two colloidal particles are far away from each other, that is, $E \gg a$, we may use the far field expansion of the diffusion tensor. Moreover, if the two particles are restricted to moving within small ranges, the argument $\boldsymbol{r}_2-\boldsymbol{r}_1$ can be substituted by $E\hat{\boldsymbol{x}}$, so that Eqs.(15) reduces to a set of linear stochastic differential equations, the formal solution of which can easily be obtained. For an infinitely long time, we write out the time-correlation functions of the colloidal particles, through using Eqs.(16), as

$$\begin{aligned}
\left\langle r_1^\alpha(t) r_1^\beta(t')\right\rangle &= \left\langle \left(r_2^\alpha(t)-E\right)\left(r_2^\beta(t')-E\right)\right\rangle = \delta_{\alpha\beta}\frac{k_\mathrm{B}T}{k}\left(\mathrm{e}^{-|t-t'|(1+\varepsilon_\alpha)/\tau_\alpha}+\mathrm{e}^{-|t-t'|(1-\varepsilon_\alpha)/\tau_\alpha}\right), \\
\left\langle r_1^\alpha(t)\left(r_2^\beta(t')-E\right)\right\rangle &= \left\langle \left(r_2^\alpha(t)-E\right) r_1^\beta(t')\right\rangle = \delta_{\alpha\beta}\frac{k_\mathrm{B}T}{k}\left(\mathrm{e}^{-|t-t'|(1+\varepsilon_\alpha)/\tau_\alpha}-\mathrm{e}^{-|t-t'|(1-\varepsilon_\alpha)/\tau_\alpha}\right).
\end{aligned} \tag{17}$$

When utilizing Oseen tensor, the parameters in Eqs.(17) are $\tau_x = \tau_y = \tau_z = \frac{6\pi\eta a}{k}$, $\varepsilon_x = \frac{3a}{2E}$, and $\varepsilon_y = \varepsilon_z = \frac{3a}{4E}$, respectively. In the experiment of Meiners and Quake[6], E is set between 2 and 15 μm, the radius of the colloidal particle $a = 0.5\,\mu$m and each particle moves within the range of 16 nm; therefore Eqs.(17) is expected to be in good agreement with the experimental results. Accordingly, we can also use the more accurate far field expansion to obtain the expressions of τ_a and ϵ_a.

3. Simulation results and analysis

In this section, we present the numerical results obtained by means of Brownian dynamics simulation of two confined colloidal particles. As mentioned above, we compare the results calculated from the accurate diffusion tensor by using Hinsen's program package with those from the approximate analytical expression (17). We calculate the displacements of the two particles for each step by using Eqs.(11), where the random displacements can be constructed by using the method proposed by Ermak and McCammon,[13] i.e. by decomposing the diffusion tensor through lower-upper (LU) decomposition method and producing the random numbers with Gaussian distribution. Let the radius of spheres be $a = 500\,$nm, and the solvent viscosity $\eta = 0.88\times10^{-3}\,\mathrm{kg/(m{\cdot}s)}$. Since the time interval should satisfy $\Delta t \gg \frac{mD_0}{k_\mathrm{B}T} \simeq 0.14\,\mu$s, we take $\Delta t = 100\times 0.14\,\mu\mathrm{s} \simeq 0.015\,$ms. Figure 2(a) shows the autocorrelation functions of the relative coordinate x between the two spheres as time varies. Since the autocorrelation function varies slightly with the distance between two particles when they are far away from each other, we present here only the autocorrelation function for the equilibrium distance $E = 4.8\,\mu$m. The solid line denotes the analytical result obtained from Eqs.(17), while the circles correspond to the result from numerical simulation. It can be seen that the

two results coincide with each other quite well, which indicates two things: one is that, the Oseen tensor is a very nice approximation to the diffusion tensor, and the other is that the differential equation approximation given by Eqs.(15) is a good approximation to the Brownian dynamics when the distances between two colloidal particles are large.

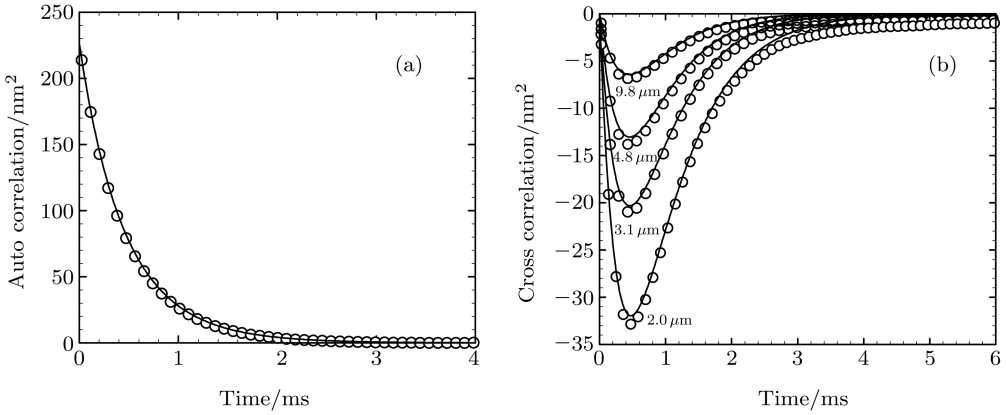


Fig.2. (a) Autocorrelation function of coordinate x of the two spheres, the equilibrium positions of which are set 4.8 μm apart. (b) Cross-correlation function of coordinate x of two spheres held at a separation of 9.8 μm, 4.8 μm, 3.1 μm, and 2.0 μm, respectively. In both calculations the Oseen formula is utilized to approximate the diffusion tensor. The solid line denotes the result from approximate analytical expression, while the circle corresponds to result from numerical simulation.

We present the crosscorrelation functions of two particles in the x-direction as time varies for a few equilibrium distances in Fig.2(b). Similarly, the solid line denotes the result calculated from Eqs.(17), while the circle corresponds to the result from numerical simulation. It can be seen that the two results are quite close to each other up to the situation where the distances between two colloidal particles are twice the diameter. Moreover, the two results have very small deviations from each other when the two particles turn closer.

In order to find the influence of different expansion forms of the diffusion tensor on the calculation and the validity of the approximate differential equation, we compute the correlation function with the approximate analytical expression (17) by utilizing Oseen tensor, Rotne–Prager tensor and the formula expanded to order $\frac{1}{r^7}$, separately. Furthermore, we compare these results with those obtained from Brownian dynamics simulation with the accurate diffusion tensor obtained from the numerical package as shown in Fig.3. When two particles are very close to each other, e.g. $E = 1.1\,\mu$m, the calculation result using approximate analytical formula (17) deviates obviously from that of Brownian dynamics simulation (see Fig.4). The reason lies in the fact that the two preconditions which lead to the analytical formula are

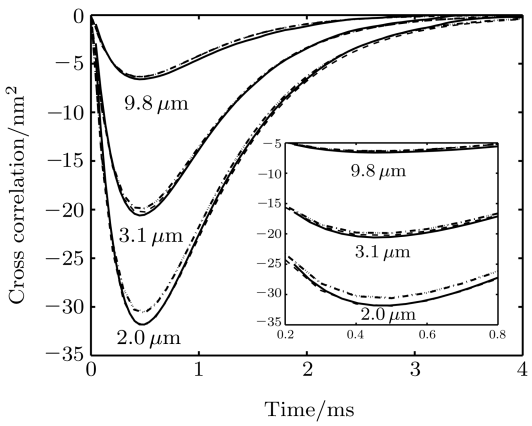


Fig.3. Comparison of cross-correlation function of coordinate x obtained from the approximate analytical expression with the numerical simulation results by using the accurate diffusion tensor. The equilibrium positions of two spheres are set at a separation of 9.8 μm, 3.1 μm, and 2.0 μm, respectively. Dashed line, dotted line and dot-dashed line represent the results using approximate analytical formulae, i.e. Oseen tensor, Rotne–Prager tensor and the formula expanded to order $\frac{1}{r^7}$, respectively, while solid line denotes the numerical simulation result using the accurate diffusion tensor. Inset is the enlargement of the bottom part of the curves.

no longer satisfied. However, the experimentally interesting range of the separation of the two confined colloidal spheres is much larger than twice the diameter of the sphere. Our computations show that the approximate analytic formula can well be applied. Explicitly, the relevant parameters can be obtained from

the far field formula expanded to order $\frac{1}{r^7}$, which assures the accuracy of the computational results. In this way, we acquire a formula which fits the experimental data quite well. On the contrary, as the interparticle distance becomes less than twice the sphere diameter, the calculation error becomes larger and accordingly the analytical formula cannot be used to fit the experimental data.

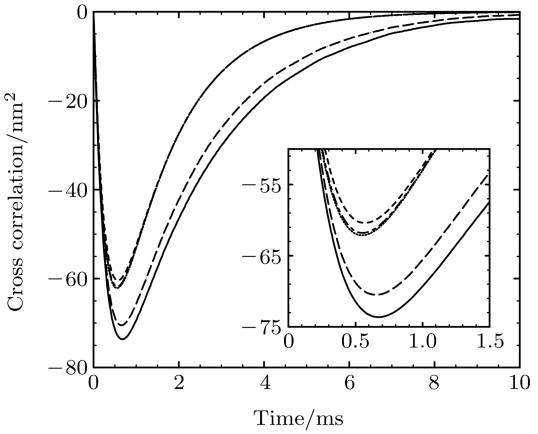


Fig.4. Comparison of cross-correlation function of coordinate x obtained from the approximate analytical expression with the numerical simulation results obtained by using the accurate diffusion tensor. The equilibrium positions of two spheres are 1.1 μm apart. Dashed line, dotted line and dot-dashed line represent the results obtained using approximate analytical formulae, i.e. Oseen tensor, Rotne-Prager tensor, and the formula expanded to order $\frac{1}{r^7}$, respectively. Solid line and long-dashed line denote the numerical simulation result obtained by using the accurate diffusion tensor and the formula expanded to order $\frac{1}{r^7}$, respectively. Inset is the enlargement of the bottom part of the curves.

The most distinct feature of the crosscorrelation function is that it exhibits anticorrelation, and there is a minimum in the correlation function. By using the approximate analytic formula, we obtain the time corresponding to the minimum point as

$$|t - t'|_{\min} = \tau_x, \tag{18}$$

while the minimum value is

$$\begin{aligned} &\langle r_1^x(t)(r_2^x(t') - E)\rangle_{\min} \\ &= -\frac{1}{e}\frac{k_{\mathrm{B}}T}{k}\varepsilon_x \\ &= -\frac{1}{e}\frac{k_{\mathrm{B}}T}{k}\frac{3}{2}\frac{a}{E} + O\left(\frac{a}{E}\right)^2. \end{aligned} \tag{19}$$

Obviously, the minimum of cross-correlation function varies linearly with a/E when the particles are far away from each other. Figure 5 shows the relation between the minimum value of the cross-correlation function and a/E obtained from formula (19) and from numerical simulation, respectively. For a comparison, we also include here the experimental result obtained by Meiners and Quake.[6] The deviation of the experimental result from the theoretical computation may come from the fact that the harmonic potential does not describe the real binding potential in this situation. Using the relations (18) and (19), one can measure the rheological properties of the fluids by measuring the crosscorrelation function and locate its minimum.

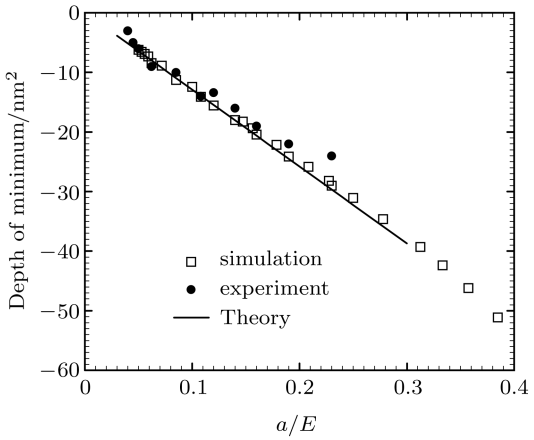


Fig.5. The relation of the minimum value of the cross-correlation function of coordinate x to a/E. The solid line represents the result calculated by using Eq.(19), the square corresponds to the Brownian dynamics simulation result, while the filled circle corresponds to the data obtained from experiment by Meiners.

4. Conclusion

We have studied the hydrodynamical behaviour of two confined colloidal particles in the suspension by means of Brownian dynamics simulation, which gives the accurate numerical result. We have also examined various approximate analytical results, and obtained the conditions under which each approximation can be applied. Furthermore, the above results are compared with the experimental data from Ref.[6]. This model of two confined particles is already realized in experiments, which can further be used to explore some more dynamical properties of biological systems. In this sense the formulae which lead to the approximate analytical results presented here and the relevant conditions are useful to experimental research.

References

[1] Ayton G, Tepper H, Mirijanian D and Voth G 2004 *J. Chem. Phys.* **120** 4074

[2] Reichert M and Stark H 2004 *Phys. Rev.* E **69** 031407

[3] Urbina-Villalba G, García-Sucre M and Toro-Mendoza J 2003 *Phys. Rev.* E **68** 061408

[4] Yang T, He D H, Zhang Q L and Ma H R 2005 *Acta Phys. Sin.* **54** 5937 (in Chinese)

[5] Henderson S, Mitchell S and Bartlett P 2001 *Phys. Rev.* E **64** 061403

[6] Meiners J and Quake S 1999 *Phys. Rev. Lett.* **82** 2211

[7] Xu S H, Li Y M, Lou L R and Sun Z W 2005 *Chin. Phys.* **14** 382

[8] Guo J Y, Huang L X and Xiao C M 2006 *Chin. Phys.* **15** 1638

[9] Wang X D, Dong P and Yi G L 2006 *Acta Phys. Sin.* **55** 2092 (in Chinese)

[10] Liu L, Xu S H, Liu J, Duan L, Sun Z W, Liu R X and Dong P 2006 *Acta Phys. Sin.* **55** 6168 (in Chinese)

[11] Mazo R 1969 *J. Stat. Phys.* **1** 559

[12] Deutch J M and Oppenheim I 1971 *J. Chem. Phys.* **54** 3547

[13] Ermak D and McCammon J 1978 *J. Chem. Phys.* **69** 1352

[14] Jeffrey D and Onishi Y 1984 *Z. Angew. Math. Phys.* **35** 634

[15] Kim S and Karrila S 1991 *Microhydrodynamics: Principles and Selected Applications* (Butterworth-Heinemann Stoneham, MA)

[16] Hinsen K 1995 *Computer Physics Communications* **88** 327